Poster: #020

Geometry of the GNSS Beam and Absolute Value of the Galileo Satellite Phase Center Offset

Drazen Svehla

ABSTRACT

From SLR measurements we know that Gaussian beam divergence of laser light is a function of beam diameter and wavelength. After decreasing the beam radius of the transmitted laser beam from the LEO orbit to GNSS satellites, we can show that thanks to laser beam divergence, despite the huge satellite velocity in LEO orbit, LEO-to-GNSS and LEO-to-ground laser interferometry is feasible in the LEO orbit, either to the SLR corner cubes placed on-board GNSS satellites or to the SLR corner cubes placed on the ground (what we call "laser DORIS" or "laser PRARE"). Here we show that Gaussian beam divergence can also be extended to GNSS where, due to the huge GNSS wavelength in L-band (compared to laser SLR at 532-1064 nm), GNSS can illuminate the entire Earth's disk. We show that GNSS beam divergence in L-band corresponds to the diameter of the inner Galileo (or GPS) satellite antenna that radiates the main signal power towards the Earth, whereas the outer satellite antenna fulfills the isoflux coverage condition for the Earth's disk.

Thanks to this GNSS beam divergence in L-band, we show that there is another effect called the Gouy phase shift effect associated with beam divergence (and beam convergence) that is reported from optical (laser), microwave to acoustic waves. Due to the divergence of the GNSS beam, transmitted carrier-phase measurements are shifted in phase by (n+1)×π/2, where "n" is an integer number derived from the beam shape. Sign of the effect depends on the electric field phasor convention (RHCP) and the effect is a cosine function of a nadir angle. This phase shift effect is used in the analytical modelling of optical (laser) and microwave beams, where such a beam is typically associated with the Gaussian beam in both frequency bands and can form different higher-order modes or the shape of the transmitted power.

Recently, DLR carried out measurements of the Galileo satellite antenna gain by making use of the 30 m high-gain, deep-space antenna at the Weilheim ground station and confirmed the 'donut' shape of the Galileo satellite antenna gain, similar to GPS. This 'donut shape' of the Galileo satellite antenna gain indirectly confirms (n=3) that the phase shift effect gives exactly one narrow-lane wavelength when the ionosphere-free linear combination is formed between E1 and E5a Galileo carrier-phase measurements (or L1 and L2 for GPS). This missing narrow-lane wavelength in the Galileo/GNSS measurements corresponds very well in size and sign with an estimated bias in the Galileo satellite phase center offset reported at -11.6 cm in satellite nadir direction (w.r.t. calibrated value) based on the GNSS measurements from the IGS network. After correcting the Galileo satellite antenna phase center offset in the nadir direction, this phase shift effect for carrier-phase measurements (10.9 cm for E1/E5a) reduces the bias in the scale of the GNSS terrestrial reference frame by 0.70 ppb for Galileo (E1/E5a) and 0.69 ppb for GPS (L1/L2) and brings the scale of the GNSS terrestrial reference frame down to the scale of the terrestrial reference frame estimated by SLR and VLBI, which already agree at 0.15 ppb.

SLR and GNSS Beam Geometry

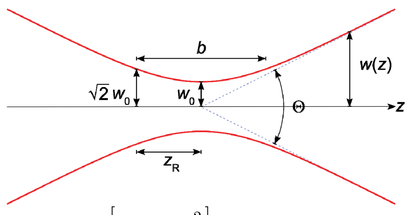

Radius of beam curvature $R(z) = z\left[1+\left(\frac{z_R}{z}\right)^2\right]$

Rayleigh range $z_R = \frac{w_0^2\pi}{\lambda}$

Gouy phase shift $\psi(z) = \arctan\left(\frac{z}{z_R}\right) \doteq \frac{\pi}{2}$ for $z \gg 0$

Beam divergence $\theta = \frac{\Theta}{2} = \frac{\lambda}{\pi\omega_0}$ — wavelength; beam radius (beam waist)

Galileo Gouy Phase Shift Along the Nadir Axis

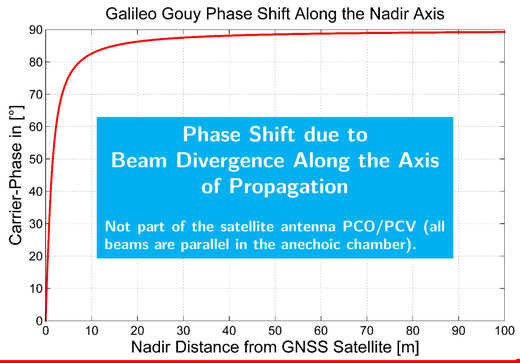

The Gouy phase shift is an increase in the carrier-phase or a phase shift near the beam waist (z≈0) due to convergence or divergence (GNSS) of the beam. Thus the phase velocity formally exceeds the speed of light along the axis of propagation of the beam. The sign of the Gouy phase shift depends on the sign convention chosen for the electric field phasor. With $e^{i\omega t}$ dependence, the Gouy phase changes from -π/2 (or 0° for a transmitter) to +π/2, while with $e^{-i\omega t}$ dependence it changes from +π/2 to -π/2 (or 0°) along the axis.

SLR and GNSS Beam Divergence

For SLR the beam divergence is only 0.14"-1.4" (20-200 m) due to a small laser wavelength

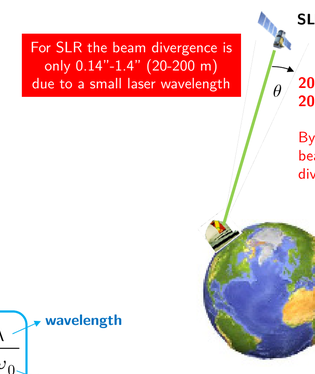

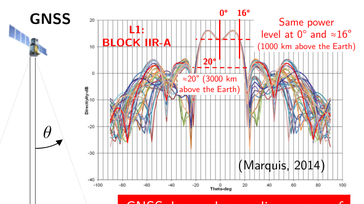

GNSS has a beam divergence of about 16° and the calculated size of the GNSS antenna confirms that as well as the published dB directivity figures (GPS). The 16° corresponds to height of about 1000 km above the Earth and the signal power rapidly drops up to the height of 3000 km (GPS)..

$\theta_{SLR}(532\text{ nm}) = \frac{532\text{ nm}}{\pi\cdot 0.25\text{ m}}\cdot 29600\text{ km} = 20\text{ m}$

$\theta_{SLR}(532\text{ nm}) = \frac{532\text{ nm}}{\pi\cdot 0.025\text{ m}}\cdot 29600\text{ km} = 200\text{ m}$

$\theta_{SLR}(1064\text{ nm}) = \frac{1064\text{ nm}}{\pi\cdot 0.25\text{ m}}\cdot 29600\text{ km} = 40\text{ m}$

$\theta_{SLR}(1064\text{ nm}) = \frac{1064\text{ nm}}{\pi\cdot 0.025\text{ m}}\cdot 29600\text{ km} = 400\text{ m}$

Beam radius for Galileo at 29 600 km

$\omega_0(E1) = 19$ cm

$\omega_0(E6) = 25$ cm → Inner Antenna Size ∅50 cm

Beam Radius for GPS at 26 553 km

$\omega_0(L_1) = 22$ cm

$\omega_0(L_5) = 29$ cm → Inner Antenna Size ∅58 cm

The main GNSS signal power is radiated by the inner antenna (∅50-60 cm) and its size matches the antenna size calculated from the beam divergence (Galileo, GLONASS, GPS). The outer antenna is used for the isoflux condition.

Outer ∅1.20 m/Inner ∅0.50 m — ∅ 1.20 m (Schmitz et al., 2008)

Impact of the Combined JASON-2 Orbit (GPS+SLR+DORIS) on GPS Orbits

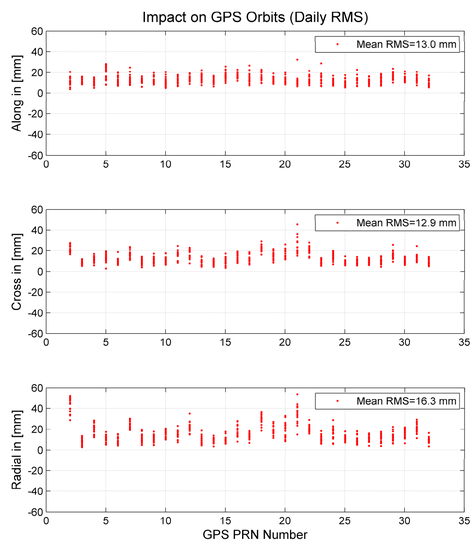

Dominated orbit component: NOT the along-track GENESIS is not going to improve GNSS satellite orbits

VLBI in L-Band with GNSS in ICRF Geometry Beam Application #1

Proposed an ICRF extension to L-Band

by estimating ICRF quasar coordinates in L-band relative to official X/S-band quasar positions, every 3 weeks for a set of good quasars (AGNs)

GNSS Orbits in ICRF

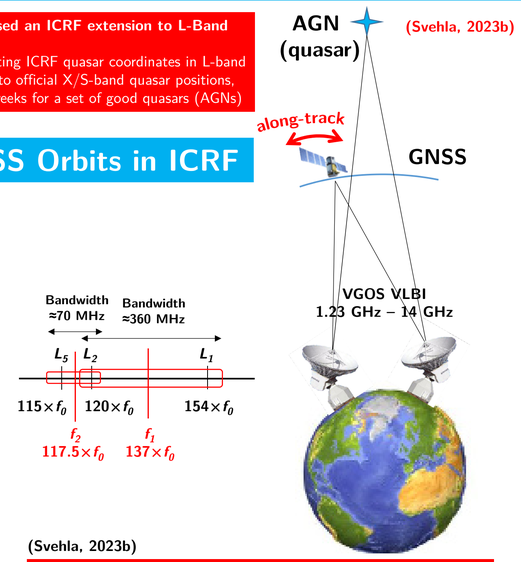

(Svehla, 2023b)

PROPOSAL to IVS (confirmed by Ch. Jacobs - JPL):
To observe with VLBI a set of good AGNs (quasars) in L-band relative to their X/S-band positions (e.g. every 3 weeks) and try to improve the along-track orbit component of GNSS satellites

LEO-to-GNSS Laser Interferometer Geometry Beam Application #2

Single-differences formed between two GRACE satellites - to remove orbit and signature effects of the SLR reflector onboard a GNSS satellite

Noise level <1 μm with IGS orbits (CODE-JPL)

"Vertical" GRACE

LEO beam divergence increased by ×6 (due to LEO velocity aberration)

→ LEO transmitted beam ∅ 5 cm (100 W)

Received beam: ∅ 30 cm (2.5 pW)

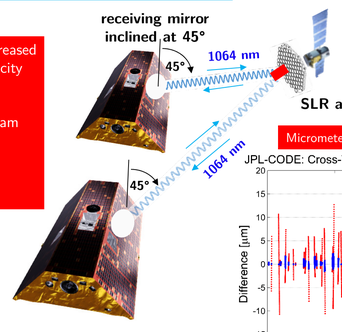

Micrometers with IGS orbit (over 5 min)

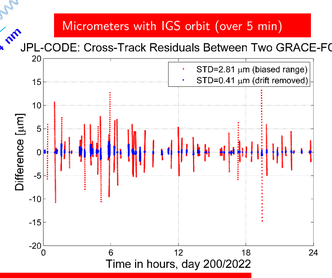

(Svehla, 2023a)

Simulation of the "Vertical GRACE" concept with GPS Orbits (JPL-CODE): Simulated single-difference biased range between two GRACE-FO satellites in cross-track (receiving mirror inclined at 45° with tracking antenna zenith angle of 10° → 5 minute tracking passes). Antenna zenith angle of 10°-15° gives 4-6 minute tracking passes. The STD=2.8 μm (for zenith angle 15°, STD=4.6 μm) is reduced to STD=0.41 μm by removing a linear drift. One can get STD=12 nm by removing a quadratic fit (STD=45 nm for the antenna zenith angle of 15°).

"Laser DORIS"

optical cross-section:

$\sigma_{cc} = \frac{\pi^3\rho D^4}{4\lambda^2}$

ρ = corne-cube reflectivity: 0.78 – 0.93

D = corner-cube diameter

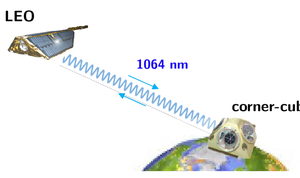

(Svehla, 2023a)

Link budget of the "laser DORIS" concept or "laser PRARE" using a single ground corner-cube reflector with a diameter of 38 mm, 2×38 mm and 3×38 mm. For the transmitted laser power of 30 W (only a 2.5-cm transmitted beam diameter), received power of 1.0 nW (5 cm diameter) is the same as the received laser power onboard the GRACE-FO mission (1 nW).

Transmitted beam:
Diameter = 2.5 cm
Power = 30 W

Received beam:
Diameter = 5 cm
Power = 1.0 nW (GRACE-FO)

Gouy Phase Shift Geometry Beam Application #4

Gaussian beam

$E(r,z) = E_0\frac{\omega_0}{\omega(z)}\exp\left(-\frac{r^2}{\omega(z)^2}\right)\exp\left\{-i\left[kz + k\frac{r^2}{2R(z)} - \psi(z)\right]\right\}$

$k = \frac{2\pi}{\lambda}$, beam radius $\omega(z) = \omega_0\sqrt{1+\left[\lambda z/\left(\pi\omega_0^2\right)\right]}$

Gouy phase shift

$\psi(z) = \arctan\left(\frac{z}{z_R}\right) \doteq \frac{\pi}{2}$ for $z \gg 0$ Rayleigh length $z_R = \frac{\pi\omega_0^2}{\lambda}$

Higher-mode Gaussian beam (Laguerre-Gaussian)
"donut" beam shape (circularly symmetric)

Laguerre polynomials

$LG_p^l(r,\vartheta,z) = E_0\frac{K_{lp}}{\omega(z)}\left(\frac{r\sqrt{2}}{\omega(z)}\right)^{|l|}\times e^{-il\vartheta}e^{-\left(\frac{r^2}{\omega(z)}\right)^2}L_p^{|l|}\left(\frac{2r^2}{\omega(z)}\right)e^{-\frac{ikr^2}{2R(z)}}e^{-i(2p+|l|+1)\psi}$

(Yao, 2018)

"Donut" beam shape Generated by inner and outer antenna

Higher-Mode Gaussian Beam "Donut" Beam Shape

Gouy phase shift $\psi(z) = \left(1+2p+|l|\right)\arctan\left(\frac{z}{z_R}\right) \doteq \left(1+2p+|l|\right)\frac{\pi}{2}$

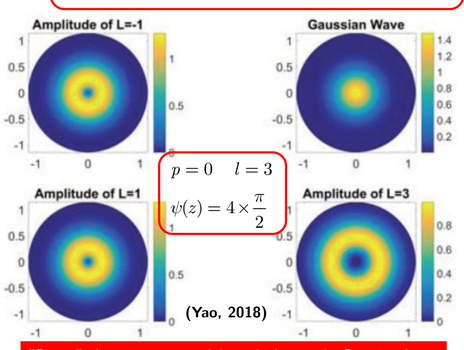

(Yao, 2018)

"Donut" shape is generated by a higher-mode Gaussian beam with l=3 (or l=1) and no radial nodes (p=0). "Donut" is generated as a superposition of inner and outer GNSS antenna.

Galileo Satellite Antenna Gain

Measured "Donut" Beam Shape

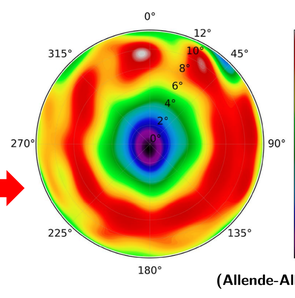

(Allende-Alba et al., 2020)

Reconstructed antenna gain in the E5 band for satellite GSAT0213 using a harmonics expansion with N = 15. The gain pattern has been normalized with the maximum gain value

High-gain 30 m deep space antenna at the DLR ground station near Weilheim, Germany

GPS Satellite Antenna Gain

GPS "Donut" Beam Shape

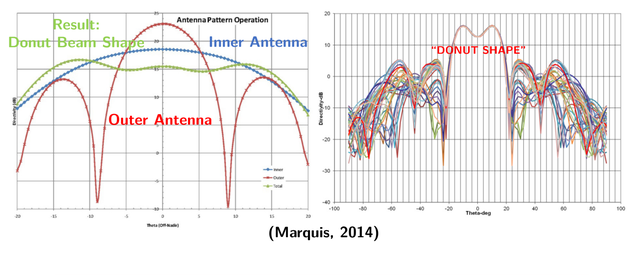

(Marquis, 2014)

GPS Block IIR: nominal satellite antenna pattern from inner antenna (blue), outer antenna (red) and the resulting "donut" beam shape (green).

Gouy Phase Shift and PCO Offset

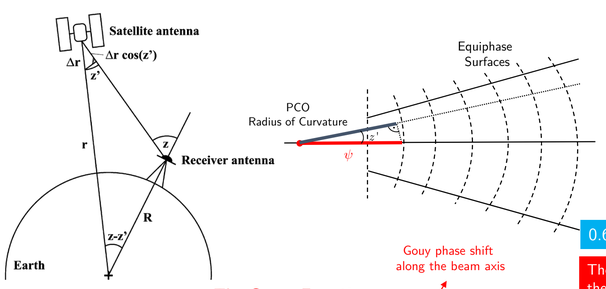

The Same Equation

$\Delta\phi(z') = -\Delta r\cdot\left(1-\cos(z')\right)$ $\Delta\phi(z') = -\psi\cdot\left(1-\cos(z')\right)$

(Schmid and Rothacher, 2003)

Gouy Phase Shift and Satellite ΔZ-PCO Offset and Scale

Linear Combination	l=1 ψ(z)	l=1 ΔZ-PCO [cm]	l=1 ΔScale [ppb]	l=3 ψ(z)	l=3 ΔZ-PCO [cm]	l=3 Δscale [ppb]
Galileo E1/E5a	π	-5.5	0.35	2π	-10.9	0.70
Galileo E1/E5b	π	-5.4	0.35	2π	-10.8	0.69
GPS L1/L2	π	-5.3	0.34	2π	-10.7	0.69

0.69 ppb (Altamimi et al. 2024): GNSS scale vs. ITRF2020 (SLR and VLBI)

The missing narrow-lane wavelength (-10.7 cm) in the Galileo/GPS Z-PCO is EXACTLY the scale difference of 0.69 ppb reported by (Altamimi et al. 2024) for the scale of the GNSS terrestrial reference frame against ITRF2020, where scale is defined by SLR and VLBI (see equation on the right).

This corresponds very well in size and sign (0.695 ppb) with an estimated bias in the Galileo satellite phase center offset reported at -11.6 cm (see Table on the right) in satellite nadir direction (w.r.t. calibrated value) based on the GNSS measurements from the IGS network (Steigenberger and Montenbruck, 2023) and reported scale of 0.68 ppb by (Schoenemann et al., 2024) between an IGS solution with the Galileo and GPS III anechoic chamber calibrations for the satellite PCO/PCV.

Estimated Galileo/GPS ΔZ-PCO Offset and Scale

Mean Z-PCO differences between estimated values and manufacturer calibrations for Galileo satellites. The last two columns give the scale differences w.r.t. ITRF2020 at epoch 2022.0 obtained from ΔZ-PCO according to enclosed quation from (Steigenberger and Montenbruck, 2023).

Linear combination	ΔZ-PCO [cm] E101/3	E102	FOC	All	ΔScale [ppb] FOC	All
E1/E5a	−14.2	−1.0	−11.6	−11.4	0.75	0.73
E1/E5b	−2.5	10.1	−11.9	−10.2	0.77	0.66
E1/E6	−11.1	2.6	−15.7	−14.5	1.01	0.93

(Steigenberger and Montenbruck, 2023)

GNSS Scale and ΔZ-PCO Offset $\alpha = \frac{\Delta h}{\Delta PCO_z} = -0.041$

0.69 ppb = ΔZ-PCO=-10.7 cm = Δh=4.5 mm

References

Allende-Alba G., Thoelert S. (2020) Reconstructing antenna gain patterns of Galileo satellites for signal power monitoring. GPS Solutions 24:22, https://doi.org/10.1007/s10291-019-0937-9

Marquis W (2014) The GPS Block IIR/IIR-M Antenna Panel Pattern https://www.navcen.uscg.gov/sites/default/files/pdf/gps/GPS_Block_IIR_IIR_M_Antenna_Panel_Pattern_Marquis_Aug2015_revised.pdf

Schmid, M. Rothacher (2003) Estimation of elevation-dependent satellite antenna phase center variations of GPS satellites. Journal of Geodesy (2003) 77: 440–446 DOI 10.1007/s00190-003-0339-0

Schmitz, M., Wübbena, G., Propp, M (2008) Absolute Robot-Based GNSS Antenna Calibration – Features and Findings –. International Symposium on GNSS, Space-based and Ground-based Augmentation Systems and Applications, November 11-14, 2008, Berlin, Germany

Steigenberger, P., Montenbruck, O. (2023) Consistency of Galileo satellite antenna phase center offsets. J Geod 97, 58. https://doi.org/10.1007/s00190-023-01750-0

Svehla D, Rothacher M, Hugentobler U, Nothnagel A, Willis P, Biancale R, Ziebart M, Appleby G, Schuh H, Adam J, Iess L and Cacciapuoti L (2014) Terrestrial and Celestial Reference Frame Realization with Highly Elliptical Orbit - The ESA STE-QUEST Mission. Geophysical Research Abstracts, Vol. 16, EGU2014-7934-2

Svehla D (2018) Geometrical Theory of Satellite Orbits and Gravity Field, Springer Theses, Springer Nature, 537 pages, DOI https://doi.org/10.1007/978-3-319-76873-1

Svehla D (2023) LEO-to-GNSS Laser Interferometer for Space Geodesy with Laser DORIS and Laser SAR EGU General Assembly, Vienna, 23-28 April 2023.

Svehla D (2023) Proposal to IVS: Extension of the ICRF Frame to L-Band for the Observation of GNSS Constellations in the Celestial Frame. EVGA 2023, Bad Kötzting, 11-15 June 2023, https://doi.org/10.5281/zenodo.8, https://zenodo.org/record/8077211

Yao H (2018) Radio-frequency Communication Using Higher Order Gaussian Beams. PhD Thesis, The University of Texas at Dallas.

Acknowledgement:

TU München for the conference travelling cost and

IGS for the conference participation fee.